IEEE Access
Multidisciplinary | Rapid Review | Open Access Journal

Received 28 February 2023, accepted 23 March 2023, date of publication 29 March 2023, date of current version 13 April 2023.

Digital Object Identifier 10.1109/ACCESS.2023.3263047

RESEARCH ARTICLE

A Dual-Polarized Broadband High Gain Base Station Antenna With an Octagonal Structure

CHENGBIN ZHANG[1], YUHUI ZHANG[2], XIWANG DAI[2], AND ZEHONG YAN[1], (Member, IEEE)

[1]Key Laboratory of Antennas and Microwave Technology, School of Electronic Engineering, Xidian University, Xi'an 710071, China
[2]School of Electronic and Information Engineering, Hangzhou Dianzi University, Hangzhou 310018, China

Corresponding author: Xiwang Dai (xwdai@hdu.edu.cn)

This work was supported in part by the Natural Science Foundation of Zhejiang Province under Contract LGG21F010007, in part by the "Pioneer" and "Leading Goose" Research and Development Program of Zhejiang under Contract 2022C01119, and in part by the National Natural Science Foundation of China under Contract 62171169.

ABSTRACT In this paper, a dual-polarized broadband high gain base station antenna unit is proposed. The antenna unit comprises an octagonal radiation structure and a pair of orthogonal Γ-shaped feeding structure, stacked patch and metal reflection structure. The octagonal radiation structure can effectively increase the radiation area, and the wide working frequency band can be realized by means of coupling and slotting. At the same time, high isolation and stable radiation pattern characteristics can be obtained. The simulation results show that the impedance bandwidth of the antenna is 47% (1.67 - 2.69 GHz) when the reflection coefficient is less than - 20 dB, and the port isolation is greater than 27 dB, a high gain of 10 ± 0.5 dBi can be obtained in the passband. Furthermore, the antenna also obtains a wide half power beam width (HPBW). The HPBW fed through a single port and two ports are around 60°. Finally, the antenna unit is applied to the 4×11 antenna array to realize the multi-band dual polarization system.

INDEX TERMS Dual-polarized, broadband, high gain, Γ-shaped feeding line, base station antenna.

I. INTRODUCTION

Due to the rapid development of communication technology, mobile communication base stations need to transmit more communication bands at the same time. In other words, the development of base station antenna can be summarized as broadband, multi-band, high gain and low cost. According to the polarization type, the base station antenna can be divided into mono polarization and dual polarization. In the design of base station antenna, if a large number of single polarization antennas are used, the number of base station antenna units will be increased, and the isolation between units needs to be considered additionally. ± 45 ° dual polarization antenna can not only ensure the isolation between units, but also reduce the number of antenna units to a great extent. For demonstration, it is widely used in the design of base station antenna.

The associate editor coordinating the review of this manuscript and approving it for publication was Mahmoud A. Abdalla.

The research on base station antenna at home and abroad has greatly promoted the development of wireless communication in recent years [1], [2], [3], [4], [5], [6], [7], [8]. These works mainly focus on the broadband characteristics of dual polarization antenna elements. A structure by introducing extra short lines at both ends of dipole arm was proposed in [1], which expanded the current flow path, additional resonance points are introduced by adjusting the coupling structure. It has stable radiation characteristics, 48% (1.64 – 2.67 GHz) impedance bandwidth and an average gain of 8.5 dBi. Similarly, two orthogonal dipoles are used to realize dual polarization in [2]. In addition, a balun is introduced between the excitation terminal and the dipole, and the impedance bandwidth of 48% (1.68–2.74 GHz) and the half-power beam width of 69 are obtained, and the average gain of 8.2 dBi is also obtained. Therefore, dual polarization antenna has a very mature application in 2GHz frequency band [10], [11], [12], [13], [14], [15], [16].

An antenna with octagonal radiation structure is proposed in this paper. It is fed by a pair of orthogonal Γ-shaped feeding

structure, and the energy is coupled to the octagonal radiation structure. The radiation structure consists of two groups of orthogonal dipole. High frequency performance is obtained by etching T-shaped slots of the octagonal radiation structure and adding an upper stacked patch. In order to further stabilize the gain of the low-frequency, several cylindrical structures are added at the edge of the radiation structure. At the same time, the cylindrical structure is folded down to reduce the physical size of the antenna. When the reflection coefficient is less than - 20 dB, it has 47% (1.67 - 2.69 GHz) impedance bandwidth and the isolation between two ports is greater than 27 dB. In this frequency band, it achieves a stable high gain of 10 $\pm$ 0.5 dBi and HPBW is about 60°. Finally, the antenna unit is further optimized, designed, fabricated and tested an array of 4 $\times$ 11 antenna units. The proposed antenna can be applied in the 2G/3G/4G/5G mobile communication systems. The working frequency covers the frequency bands of 2G (1710∼1820MHz for GSM 1880), 3G (1880-2025MHz for TD-SCDMA, 1920-2170 for CDMA 2000), 4G (1880∼2635MHz for LTE), and 5G (2515-2675MHz for China mobile) wireless communication systems.

II. ANTENNA DESIGN

The structure of a dual polarization broadband high gain base station antenna unit proposed in this paper is shown in Fig. 1. The antenna unit comprises an octagonal radiation structure and a pair of Γ-shaped feeding structure, balun, stacked patch and metal reflection structure. Four T-shaped slots and four inverted T-shaped slots are introduced on an octagonal dielectric plate to form an octagonal radiation structure. The staggered and symmetrical arrangement of the T-shaped and inverted T-shaped structures and the careful design of the slot size can not only obtain a wide HPBW and a stable radiation pattern, but also adjust the impedance matching between the antenna and the coaxial cable. Several cylindrical structures are designed on the surface of the octagonal radiation structure. The introduction of the cylindrical structure makes the gain of the antenna at the edge of the low-pass band more stable, and the physical size of the antenna can be better controlled. By adjusting the cylinder size, the working frequency band of the antenna can be further finely adjusted. The introduction of the stacked patch makes the gain curve more stable in the whole frequency band. The feeding structure adopts Γ-shaped. In the shape structure design, the two feeding lines are placed orthogonal to produce the effect of dual polarization. In order to avoid the intersection of the feeding lines, the design of one high and one low is adopted at the intersection. The edges of the two feeding lines are designed with four hollow tubes, which together form a balun. Each tube is connected with an octagonal radiation structure and a metal reflection structure to realize the conversion from the input unbalanced state of the coaxial cable to the balanced state of the radiation structure. The metal reflective structure comprises bottom plate and side plate. When the antenna is excited, the metal bottom plate can reflect electromagnetic waves, so as to enhance the directivity of the antenna. The

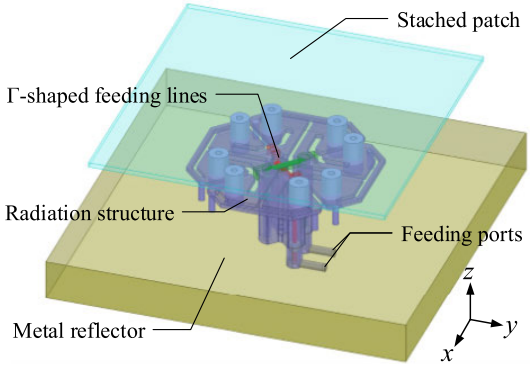

FIGURE 1. Configuration of the proposed dual-polarized broadband high gain base station antenna.

TABLE 1. Dimensions of the proposed antenna.

Parameter	ITW_1	ITW_2	TW	R_1	K_{01}	K_{02}	K_{03}	K_{04}
Value(mm)	12.00	12.00	2.40	4.25	2.00	1.20	2.00	2.35
Parameter	K_{05}	K_{06}	K_{07}	K_1	K_2	K_{11}	K_{12}	K_{13}
Value(mm)	1.20	18.75	1.40	43.80	40.75	7.90	18.30	17.70
Parameter	K_{14}	K_{15}	K_{16}	K_{21}	K_{22}	K_{23}	K_{24}	K_{25}
Value(mm)	3.70	9.00	6.85	10.00	20.10	12.70	3.50	9.00
Parameter	K_{26}	RH_1	RH_2	RH_3	KW			
Value(mm)	7.00	8.50	5.00	8.00	1.00			

metal side plate can control the HPBW and weaken the influence of electromagnetic wave diffraction on the antenna performance.

The upper dielectric substrate adopts FR4 with the size of 130 mm$\times$130 mm$\times$2 mm, and the distance from its bottom surface to the radiation structure surface is 24 mm; In the metal reflective structure, the length and width of the bottom plate are 158mm and the height of the side plate is 18mm, the overall profile of the unit is 71 mm; The octagonal radiation structure has a total width of 77 mm and a thickness of 2 mm. The detailed dimensions are given in Fig. 2. In the octagonal radiation structure, T1, T2, T3 and T4 are T-shaped slots with arm width of 2 mm, slot body width (TW) of 2.4 mm and distance between slots arms of 12.5 mm; IT1, IT2, IT3 and IT4 are inverted T-shaped slots.

The arms are composed of two rectangles (12 mm $\times$ 3.3 mm) placed at 45° and a 12 mm $\times$ 3.5 mm rectangle, the slot body is 2.5 mm $\times$ 22 mm rectangle; T-shaped slots and inverted T-shaped slots are set cross increases the effective length of vibrator arm and expands the path of current flow. Three sizes of cylindrical structures are designed under the octagonal radiation structure: hollow cylinders with inner diameter and outer diameter of 1.5 mm and 4.25 mm and height of 5 mm respectively, and a solid cylinder with a diameter of 1.4 mm and height of 8 mm. Hollow cylinders with an inner diameter of 1.5 mm and an outer diameter of 4.25 mm and a height of 8.5 mm is arranged above. Changing the size of the cylinder can not only change the width of the antenna working frequency band, but also stabilize the gain characteristics of the lower sideband edge. The same as octagonal radiation structure, symmetrical layout design is adopted when considering cylindrical distribution, so as to

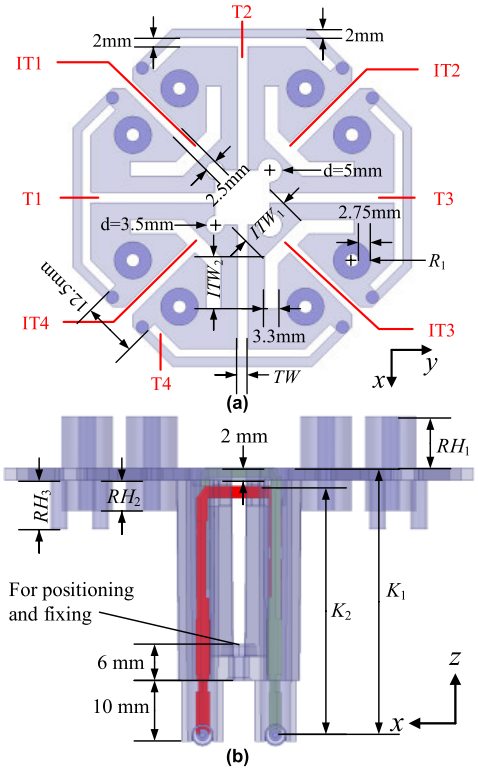

FIGURE 2. Octagonal radiation structure of the proposed dual-polarized broadband high gain base station antenna. (a) Top view. (b) Side view.

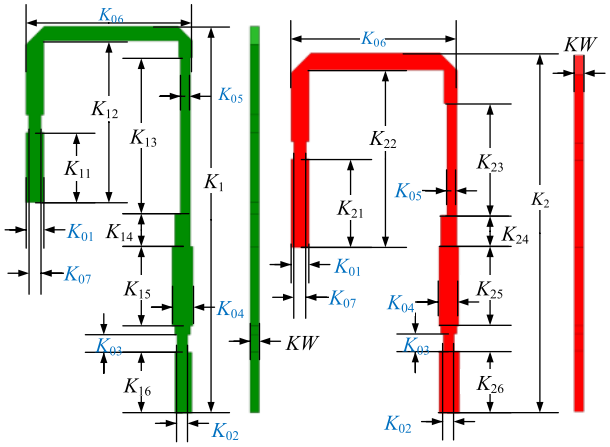

FIGURE 3. Γ-shaped feeding structure of the proposed dual-polarized broadband high gain base station antenna.

obtain more stable radiation characteristics. Γ-shaped feeding structure is shown in Fig. 3. It is composed of strip lines with different widths. The open end couples the electromagnetic energy to the octagonal radiation structure by coupling.

III. ANTENNA MECHANISM

The antenna structure is simulated and optimized by electromagnetic simulation software HFSS (High Frequency Structure Simulator). A dual polarization broadband high gain base station antenna unit proposed in this paper can

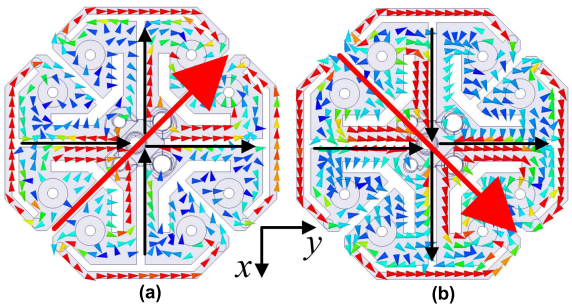

FIGURE 4. Current distribution at 2.2 GHz when (a) Port 1 (b) Port2 is excited.

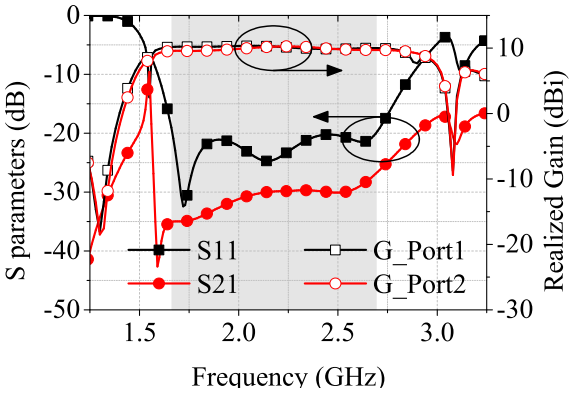

FIGURE 5. Simulated S-parameter and realized gain of the proposed antenna.

produce two kinds of polarization. When the excitation is input from Port 1, the signal is injected into Γ-shaped feeding line 1 and then coupled to the octagonal radiation structure, simulated current distribution is shown in Fig. 4(a). At this time, the current at the edges of T1 and T2 is distributed clockwise along the T-slots, and the current at the edges of T3 and T4 is distributed counterclockwise along the T-slots; The current in inverted T-slot 2 (IT2) flows from the outer arm to the inner arm, and the current in inverted T-slot 4 (IT4) flows from the inner arm to the outer arm, forming - 45° polarization. As shown in Fig. 4(b), when the excitation is input from Port 2, the current distribution is just the opposite, resulting in + 45° polarization.

Fig. 5. shows the simulated S-parameter and realized gain curve. The simulated impedance bandwidth (S11 < - 20 dB) is 47% (1.67 - 2.69 GHz), and the isolation between the two ports is greater than 27 dB. In addition, a stable high gain of 10 ± 0.5 dBi is achieved in the whole frequency band, and the average gain fed by Port 1 and Port 2 is 10.1 dBi / 9.9 dBi, respectively. Since both Port 1 and Port 2 are fed through coupling, and the two feed lines are placed in a cross manner, in order to ensure that the two feed lines do not intersect, the height of feed line 2 is 3.05 mm shorter than that of feed line 1 in spatial design. When the energy is coupled to the octagonal radiation structure, the coupling energy of feed line 2 will be slightly less than that of feed line 1. Therefore, the average gain of Port 1 is higher than Port 2 when it is fed.

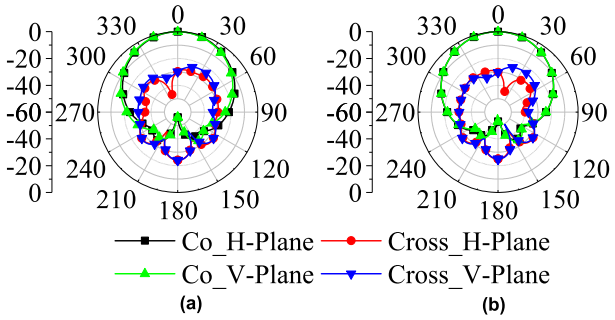

FIGURE 6. Simulated radiation patterns of the antenna at 2.2 GHz for (a) Port 1 and (b) Port 2.

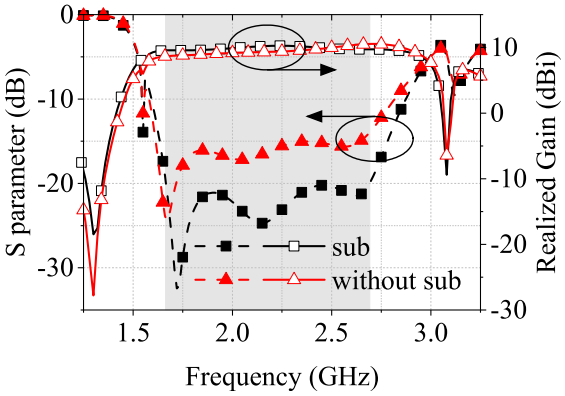

FIGURE 7. The influence of the upper substrate on S parameter and realized gain.

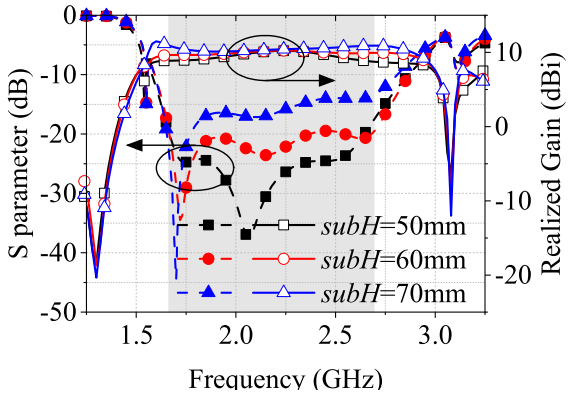

FIGURE 8. Effect of the height of the upper substrate on s parameter and realized gain.

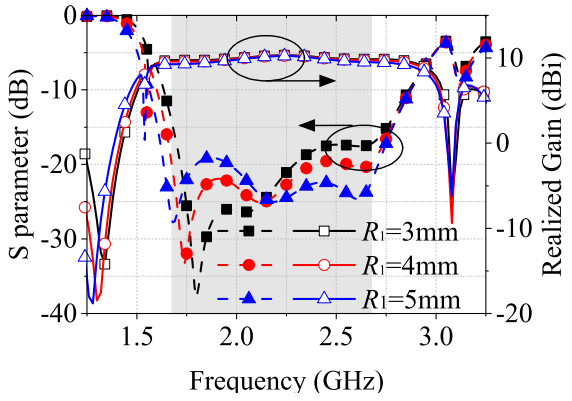

FIGURE 9. Influence of hollow cylinder external diameter R_1 on antenna parameters.

The simulation radiation patterns of only Port 1 excitation and only Port 2 excitation is shown in Fig. 6. Fig. 6(a) shows the H-plane (*xoz*-plane) and V-plane (*yoz*-plane) excited by Port 1 only at 2.2 GHz; Fig. 6(b) shows the H-plane and V-plane of Port 2 excitation only at 2.2 GHz. It is not difficult to see that when the two ports feed respectively, the co-polarization radiation patterns of H-plane and V-plane are almost the same, and the gain in the maximum radiation direction is greater than 10 dBi.

IV. PARAMETRIC STUDIES

A. INFLUENCE OF STACKED PATCH ON ANTENNA PARAMETERS

The influence of the introduction of the stacked patch on the antenna parameters is considered. Fig. 7. is a comparison diagram of S11 and realized gain with and without an upper dielectric substrate, respectively. After the introduction of the stacked patch, the impedance bandwidth increases obviously, and the S11 value in the passband moves down as a whole. Compared with the realized gain curve before the introduction of the stacked patch, the gain curve after the introduction of the stacked patch is more stable in the bandwidth, especially in the lower passband. The gain after the introduction of the stacked patch is significantly greater than that before the introduction of the stacked patch. To sum up, it can be concluded that the introduction of the stacked patch can not only increase the impedance bandwidth of the antenna to a certain extent, but also better stabilize the realized gain curve.

Next, the influence of the height of the stacked patch on the antenna parameters is considered. subH is the distance between the stacked patch and the metal reflective structure. As shown in Fig. 8. When $subH = 50$ mm, the gain in the impedance bandwidth is less than that when $subH = 60$ mm; When $subH = 70$ mm, S11 moves up as a whole and the corresponding gain increases. To a certain extent, when the height of the stacked patch becomes higher, the gain and S11 will increase. Considering the two parameters, $subH = 59$ mm is finally selected.

B. INFLUENCE OF CYLINDER SIZE ON ANTENNA PARAMETERS

Firstly, the influence of the outer diameter R_1 of the hollow cylinders on the antenna parameters is considered. As shown in Fig. 9. With the increase of R_1, the S11 value corresponding to the left resonance point increases, the frequency decreases, and the S11 value corresponding to the right resonance point decreases. Secondly, the influence of the height RH_1 of the hollow cylinders on the upper surface of the octagonal structure on the antenna parameters is considered. As shown in Fig. 10. When the height of the cylinder increases, the left and

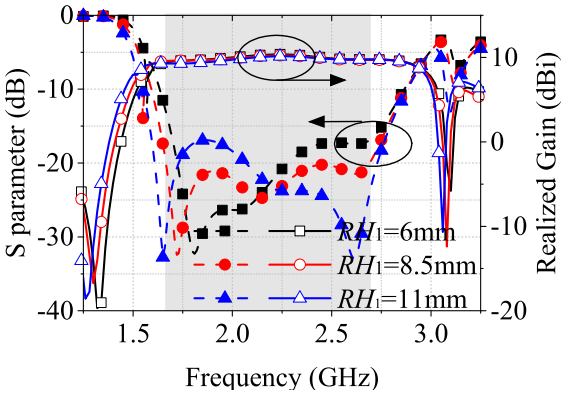

FIGURE 10. Influence of hollow cylinder height RH_1 on antenna parameters.

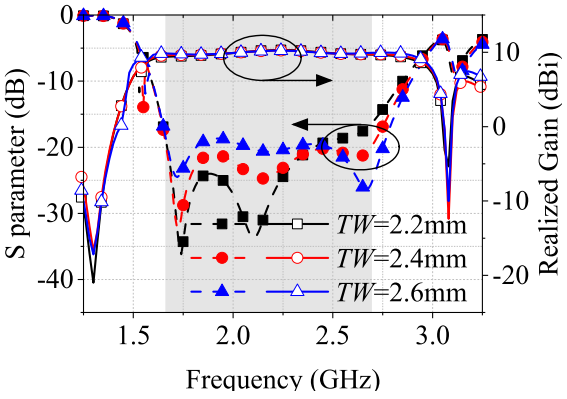

FIGURE 11. Influence of T-shaped slot body width TW on reflection coefficients.

right resonance points move to the left, and S11 corresponding to the right resonance point decreases with the increase of RH_1. When the outer diameter or height of the cylinder increases, the length of the current flow in the radiation structure also increases accordingly, the equivalent dipole arm length increases and the left resonance point moves to the low frequency direction. Therefore, the working frequency of the antenna can be adjusted more accurately by changing the size of the cylinders. The optimum bandwidth is obtained at $R_1 = 4.25$ mm and $RH_1 = 8.5$ mm.

C. INFLUENCE OF T-SLOTS AND INVERTED T-SLOTS ON ANTENNA PARAMETERS

The introduction of T-slots and inverted T-slots expands the current flow path. Therefore, the structure of T-slots and inverted T-slots are also very important to the antenna performance and antenna parameters. In order to explore the influence of inverted T-slots and T-slots on antenna parameters, we selected three parameters: T-slots body width TW and inverted T-slots two arm length ITW_1 and ITW_2. The following results are obtained through HFSS:

The width of T-slots body TW is taken as 2.2 mm, 2.4 mm and 2.6 respectively, and the S11 and realized gain curve obtained by simulation is shown in Fig. 11. In this design, the two feeding lines are not directly connected to the radiation structure, the energy reaches the radiation structure through coupling, and the width of the T-slots directly affects the degree of energy coupling to the reflecting surface. Different values of TW have a great impact on the working bandwidth of the antenna and the two resonant points in the passband. When $TW = 2.2$ mm, the impedance matching of the high-frequency part is poor, resulting in the S11 value corresponding to the right resonance point greater than -20 dB; $TW = 2.6$ mm, the impedance matching of if part is slightly poor. In addition, it can be observed that the S11 value corresponding to the left resonance point decreases with the decrease of TW, and the S11 value corresponding to the right resonance point increases with the decrease of TW. Therefore, the impedance matching of the antenna can be adjusted by adjusting the T-slots body width TW, so as to broaden the frequency band of the antenna.

Finally, the influence of the width ITW_1 and ITW_2 of the two arms of the inverted T-slots on the antenna parameters is considered, as shown in Fig. 12. and Fig. 13. respectively. ITW_1 and ITW_2 have basically the same impact on the antenna S-parameter. When the arm width increases, the current in the flow path edge of the surface of the radiation structure becomes longer, the left resonance point moves in the low frequency direction, the - 10 dB impedance bandwidth increases, and the resonance point increases when the frequency is about 2.1 GHz. Therefore, the impedance bandwidth and reflection coefficient can be adjusted by adjusting the width of the two arms of the T-slots and inverted T-slots.

D. INFLUENCE OF FEEDING LINES ON ANTENNA PARAMETERS

The coupling between the feeding lines and the radiation structure is directly related to the size of the feeding lines. It also has a great impact on the reflection coefficient of the antenna. The following will be divided into two parts: feeding lines end length K_{11} and feeding lines thickness KW to discuss the influence of feeding lines on antenna parameters.

The influence of feeding lines end length K_{11} on antenna S-parameter and realized gain is shown in Fig. 13. K_{11} here corresponds to the end branch length of feeding line 1, and the end branch length of feeding line 2 changes the same (i.e. $K_{21} = 6$ mm when $K_{11} = 4$ mm).

The design of feeding lines thickness KW is closely related to the impedance matching of antenna. As shown in Fig. 14(a). The change of feeding lines thickness KW hardly affects the gain curve of antenna, but has a great impact on S-parameters. When the feeding lines thickness is thin, the coupling degree between the two feeding lines will be reduced and better port isolation will be obtained. As shown in Fig. 14(b). In the 1.7 – 2.7 GHz frequency band, with the increase of KW, the real part of impedance increases and the imaginary part of impedance decreases. When $KW = 1$, the impedance matching degree in the whole frequency band is better.

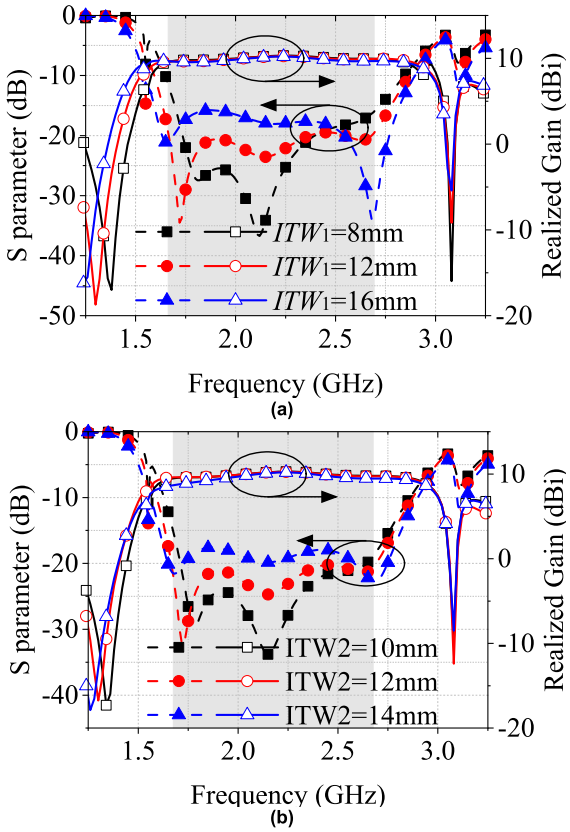

FIGURE 12. Influence of inverted T-shaped slot arm width (a) ITW_1 and (b) ITW_2 on reflection coefficients and Realized Gain.

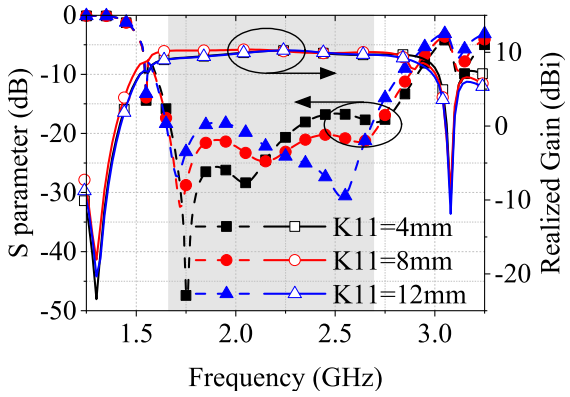

FIGURE 13. Influence of feeding line end length K_{11} on S parameter and realized gain.

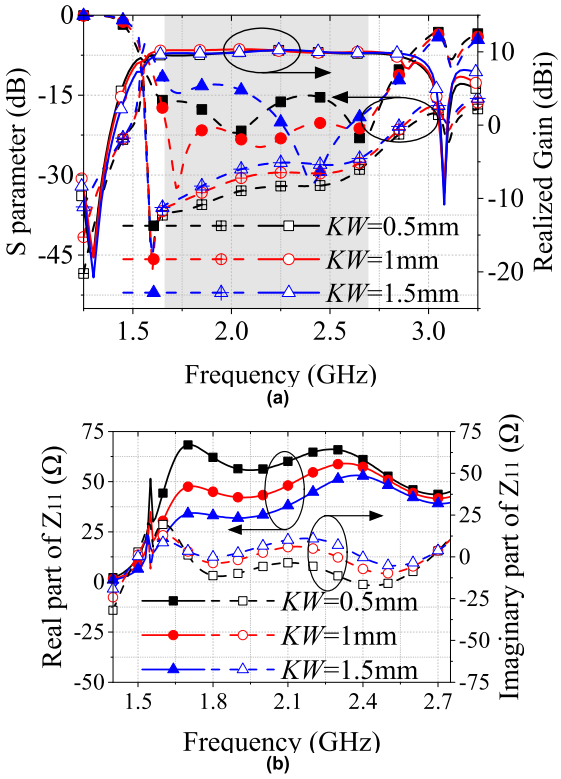

FIGURE 14. Influence of feeding line thickness *KW* on (a) S parameter and realized gain; (b) Z parameter.

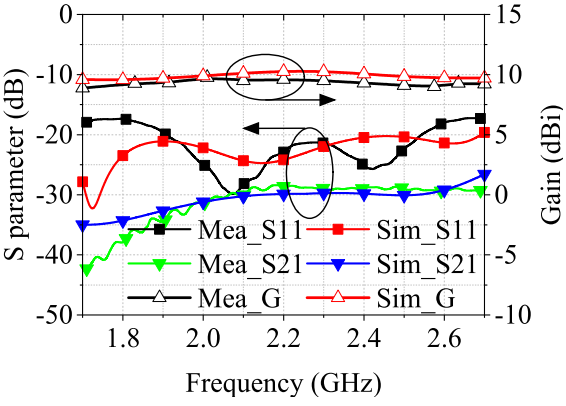

FIGURE 15. Measured and simulated S parameter and gain of the proposed antenna.

V. SIMULATED AND MEASURED RESULTS

In order to verify the structural characteristics of the antenna proposed in this paper, the antenna unit and antenna array composed of the unit covering 1.7 GHz – 2.7 GHz band is further optimized, designed and fabricated.

The measured and simulated S-parameter and Gain of antenna unit are shown in Fig. 15. In the frequency band 1.7 GHz – 2.7 GHz, the reflection coefficient (S11) of the antenna unit is less than -17 dB, the isolation between the two ports is greater than 28 dB. In addition, the average gain in the frequency band is 9.28 dBi, which can be applied to many practical communication systems.

Fig. 16. shows the radiation patterns of H-plane and V-plane measured and simulated at 1.7 GHz, 2.0 GHz and 2.6 GHz powered by Port 1. It can be observed that the radiation characteristics in the whole frequency band are relatively stable, and the half power beam width is about 65°, which shows that the antenna unit has good directivity, front to back ratio and radiation characteristics.

In order to deeply understand the antenna array composed of antenna elements, an antenna array composed of

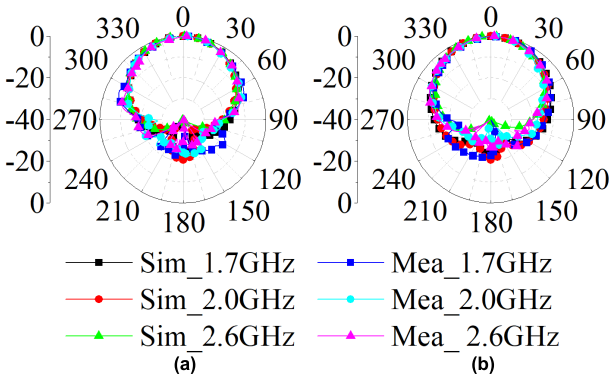

FIGURE 16. Measured and simulated radiation patterns of the antenna at 1.7 GHz, 2.0 GHz and 2.6 GHz for (a) H-Plane and (b) V-Plane.

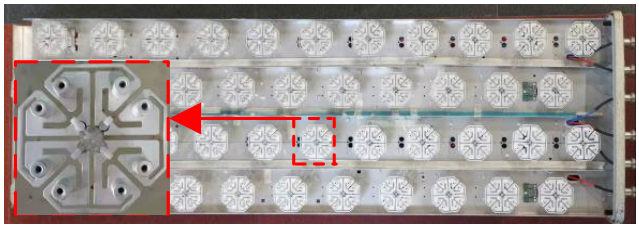

FIGURE 17. Photograph of 4 × 11 antenna array.

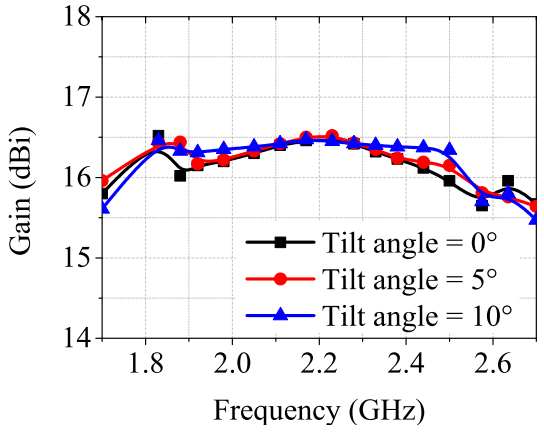

FIGURE 18. Measured gain of the 1 × 11 antenna array.

TABLE 2. Comparison of dual-polarized high gain base station antenna.

Ref.	Size (mm)	BW (%)	Polarization	ISO (dB)	Gain (dBi)
[1]	50×50	50(1.69–2.81 GHz, RL>15dB)	dual	40	8.5
[2]	61×61	48(1.68–2.74 GHz, RL>15dB)	dual	22	8.2
[3]	55×55	48.2(1.71-2.7 GHz, RL>15 dB)	dual	27.5	8.7
[4]	134×110	68(1.43-2.9 GHz, VSWR<1.5)	dual	20	8
[5]	66.3×66.3	67(1.39-2.8 GHz, RL>15 dB)	dual	30	9
[6]	62×62	72(1.32-2.82 GHz, RL>10 dB)	dual	30	8.4
[7]	120×120	169(VSWR<2.5)	single	/	2
[17]	53×53	44.5(1.710-2.69 GHz RL>15 dB)	dual	30	9.3/8.5
[18]	50×50	21(1.71–2.17 GHz RL>15 dB)	dual	28	/
This work	77×77	47(1.67–2.69 GHz, RL>20 dB)	dual	27	10 ± 0.5

44 antenna elements is designed. The array consists of array cells with column spacing of 122 mm. The array dislocation distance is set to 57.5 mm to ensure the isolation between each cell. The size of the whole array is 1392 mm × 490 mm × 156 mm. Each column contains 11 antenna units, and the spacing between each antenna unit is 115 mm, as shown in Fig. 17.

To obtain different electron-tilt angles, it is achieved by designing the phase delay of the feed network to the feed port of each array unit. When the tilt angle is 5°, from left to right, the phase delay between each cell decreases by 27° per unit. Similarly, when the current tilt angle is 10°, the phase delay between each cell decreases by 54° per unit.

Considering the similarity of each train of antennas, only one of them is selected to give the test data. Under different tilt angles the gain of 1 × 11 antenna array is shown in Fig. 18. We can find that the average gain in the frequency band reaches 16 dBi regardless of tilt angle = 0°, 5° or 10°, and the gain is relatively stable in the whole frequency band. Fig. 19. are far-field radiation pattern of the first array unit at 2110 MHz. Among them, Fig. 19(a) shows the simulated radiation pattern of H-plane under different tilt angles when feeding through Port 1 and Port 2, Fig. 19(b) shows the simulated radiation pattern of V-plane when through Port 1 and Port 2, Figs. 19(c) and (d) shows the measured radiation pattern of H-plane and V-plane when feeding through Port 1 and Port 2, and the tilt angles of the antenna array are set to 0°, 5° and 10° respectively. We can see that the main lobe direction of the radiation pattern on H-plane changes with the tilt angles, and the HPBW is 6 ± 1°, which shows that the antenna array can be applied to different use scenarios, the radiation direction can change with the tilt angles set by the user, and the directivity coefficient of the antenna array is high. The radiation pattern of the V-plane does not change with the change of the tilt angles. The HPBW in the working frequency band is 65 ± 5°, and the measured cross polarization ratio in the 0° direction is greater than 15 dB, which shows that the radiation characteristics and cross polarization characteristics of the antenna array are good and can be applied to the design of the base station antenna.

Some published papers were selected to compare the performance of antennas, which is listed in Table 2. Our work doesn't have advantage in size. However, the proposed octagonal structure shows more stable performance, such as return loss more than 20 dB and a gain of 10 dBi with a variation less than 0.5 dB. Comparing with the paper [1], [2], [3], they have the similar bandwidth, while our work has a higher gain. The structure in [7] has a wider BW of 169 for VSWR<2.5,

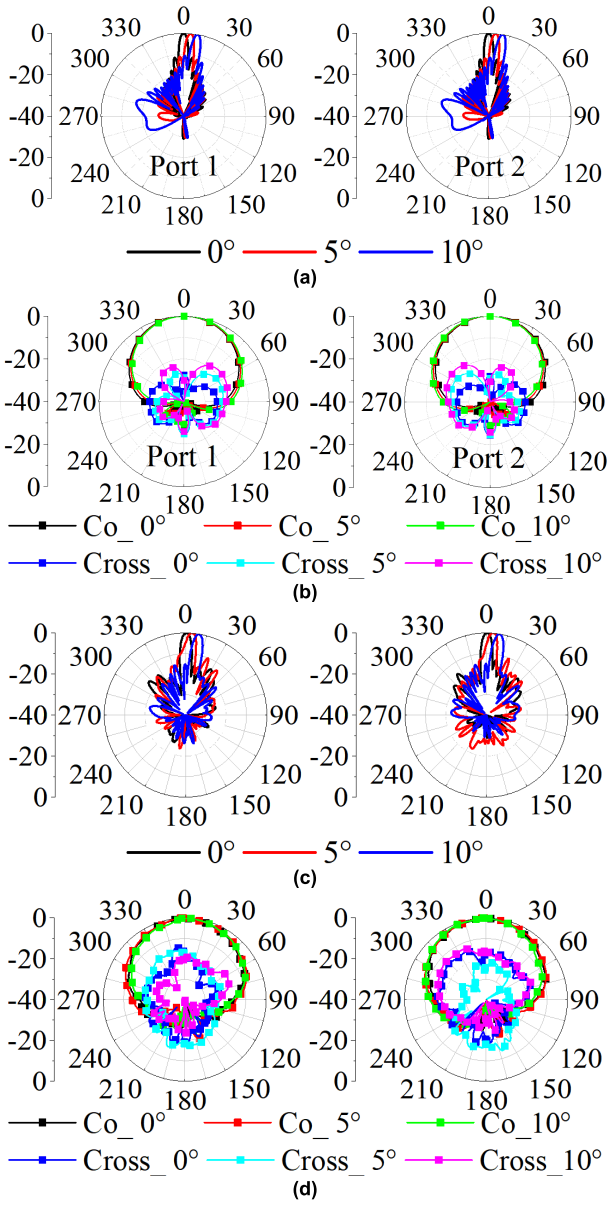

FIGURE 19. Simulated and measured radiation patterns of the 1 × 11 antenna array (a) Sim_H-Plane, (b) Sim_V-Plane, (c) Mea_H-Plane, (d) Mea_V-Plane.

however, it is only single polarization. Comparing with the structure in [17] and [18], our work exhibits a wider BW and a higher gain. The proposed structure has a potential application in wireless communication system due to its dual polarization, broad band and higher gain.

VI. CONCLUSION

A dual polarization broadband high gain base station antenna is studied in this paper. The antenna unit comprises an octagonal radiation structure and a pair of Γ-shaped feeding structure, balun, stacked patch and metal reflection structure. When the reflection coefficient is less than - 20 dB, the antenna unit has an impedance bandwidth of 47% (1.67 - 2.69 GHz), a high isolation of 27 dB between two ports, and achieves a stable high gain of 10 ± 0.5 dB and HPBW about 60°. Finally, the antenna unit and antenna array composed of the unit covers 3G and 4G frequency bands is further optimized, designed and fabricated with isolation up to 28 dB and average gain of 16 dBi in the frequency band. Therefore, a dual polarization broadband high gain antenna proposed in this paper can be used in modern wireless communication systems.

REFERENCES

[1] C. Wang, Y. Chen, and S. Yang, "Design of a compact wideband dual-polarized base-station antenna with stable radiation patterns," in *Proc. IEEE Int. Symp. Antennas Propag. USNC/URSI Nat. Radio Sci. Meeting*, vol. 2018, pp. 1365–1366.

[2] H. Huang, Y. Liu, and S. Gong, "A broadband dual-polarized base station antenna with sturdy construction," *IEEE Antennas Wireless Propag. Lett.*, vol. 16, pp. 665–668, 2016.

[3] H. Huang, Y. Liu, and S. Gong, "A dual-broadband, dual-polarized base station antenna for 2G/3G/4G applications," *IEEE Antennas Wireless Propag. Lett.*, vol. 16, pp. 1111–1114, 2017.

[4] Q. Zhang and Y. Gao, "A compact broadband dual-polarized antenna array for base stations," *IEEE Antennas Wireless Propag. Lett.*, vol. 17, no. 6, pp. 1073–1076, Jun. 2018.

[5] Y. Cui, L. Wu, and R. Li, "Bandwidth enhancement of a broadband dual-polarized antenna for 2G/3G/4G and IMT base stations," *IEEE Trans. Antennas Propag.*, vol. 66, no. 12, pp. 7368–7373, Dec. 2018.

[6] C. Wu, J. Qiu, N. Wang, O. Denisov, S. Qiu, and B. Liu, "Bandwidth enhancement of broadband dual-polarized dipole antenna for 5G base station," in *Proc. IEEE 4th Int. Conf. Electron. Technol. (ICET)*, Mar. 2021, pp. 660–663.

[7] X. Quan and R. Li, "A broadband dual-polarized omnidirectional antenna for base stations," *IEEE Trans. Antennas Propag.*, vol. 61, no. 2, pp. 943–947, Feb. 2013.

[8] Z. Li, J. Han, Y. Mu, X. Gao, and L. Li, "Dual-band dual-polarized base station antenna with a notch band for 2/3/4/5G communication systems," *IEEE Antennas Wireless Propag. Lett.*, vol. 19, no. 12, pp. 2462–2466, Dec. 2020.

[9] A. A. Omar and Z. Shen, "Compact and wideband dipole antennas," in *Proc. IEEE-APS Topical Conf. Antennas Propag. Wireless Commun. (APWC)*, Aug. 2019, pp. 1–3.

[10] S. Martin-Anton and D. Segovia-Vargas, "Fully planar dual-polarized broadband antenna for 3G, 4G and sub 6-GHz 5G base stations," *IEEE Access*, vol. 8, pp. 91940–91947, 2020.

[11] H.-H. Sun, C. Ding, H. Zhu, and Y. J. Guo, "Dual-polarized multi-resonance antennas with broad bandwidths and compact sizes for base station applications," *IEEE Open J. Antennas Propag.*, vol. 1, pp. 11–19, 2020.

[12] H. Sun, C. Ding, T. S. Bird, and Y. J. Guo, "A base station antenna element with simple structure but excellent performance," in *Proc. Austral. Microw. Symp. (AMS)*, 2018, pp. 35–36.

[13] Y. Zhao, C. Rakluea, T. Hongnara, and S. Chaimool, "A compact dual-broadband multiple-input multiple-output (MIMO) indoor base station antenna for 2G/3G/LTE systems," *IEEE Access*, vol. 7, pp. 82238–82245, 2019.

[14] G.-N. Zhou, B.-H. Sun, Q.-Y. Liang, S.-T. Wu, Y.-H. Yang, and Y.-M. Cai, "Triband dual-polarized shared-aperture antenna for 2G/3G/4G/5G base station applications," *IEEE Trans. Antennas Propag.*, vol. 69, no. 1, pp. 97–108, Jan. 2021.

[15] L. Wu, R. Li, Y. Qin, and Y. Cui, "Bandwidth-enhanced broadband dual-polarized antennas for 2G/3G/4G and IMT services," *IEEE Antennas Wireless Propag. Lett.*, vol. 17, no. 9, pp. 1702–1706, Sep. 2018.

[16] R. Wu and Q.-X. Chu, "A compact, dual-polarized multiband array for 2G/3G/4G base stations," *IEEE Trans. Antennas Propag.*, vol. 67, no. 4, pp. 2298–2304, Apr. 2019.

[17] Y. He, Y. Yue, L. Zhang, and Z. N. Chen, "A dual-broadband dual-polarized directional antenna for all-spectrum access base station applications," *IEEE Trans. Antennas Propag.*, vol. 69, no. 4, pp. 1874–1884, Apr. 2021.

[18] Y. He, W. Tian, and L. Zhang, "A novel dual-broadband dual-polarized electrical downtilt base station antenna for 2G/3G applications," *IEEE Access*, vol. 5, pp. 15241–15249, 2017.

CHENGBIN ZHANG was born in Lanzhou, Gansu, China. He received the B.S. and M.S. degrees in electronic engineering from Xidian University, Xi'an, Shaanxi, China, in 2005 and 2008, respectively, where he is currently pursuing the Ph.D. degree in electromagnetic fields and microwave technology. From March 2008 to February 2014, he was the Manager of the Antenna Department, Guangdong Huisu Corporation. From March 2014 to September 2021, he was the Manager of Dongguan Yuntong Communication Technology Company Ltd.

YUHUI ZHANG was born in Longyuan, Fujian, China. He received the B.S. degree in microelectronics science and engineering from the Xiamen University of Technology, Xiamen, Fujian, China, in 2021. He is currently pursuing the master's degree with Hangzhou Dianzi University, Hangzhou, Zhejiang, China. His current research interests include broadband antenna and reflectarray antenna.

XIWANG DAI was born in Caoxian, Shandong, China. He received the B.S. and M.S. degrees in electronic engineering and the Ph.D. degree in electromagnetic fields and microwave technology from Xidian University, Xi'an, Shaanxi, China, in 2005, 2008, and 2014, respectively.

From March 2008 to August 2011, he was the Manager of the Antenna Department, Guangdong Huisu Corporation. He is currently with Hangzhou Dianzi University, Hangzhou, China. His current research interests include broadband antenna, omni-directional antenna, MIMO antenna, and low-profile antenna.

ZEHONG YAN (Member, IEEE) was born in Tianmen, Hubei, China, in 1964. He received the B.S. and M.E. degrees in electromagnetic field and microwave technology from Xidian University, Xi'an, China, in 1980 and 1984, respectively, and the Ph.D. degree from Northwestern Polytechnical University, Xi'an, in 1996. In 1984, he joined Xidian University, where he is currently a Professor with the School of Electronic Engineering. His research interests include communications antennas, antenna tracking technology, and microwave devices.